Formation of Spindle Poles by Dynein/Dynactin-dependent Transport of NuMA

Andreas Merdes,* Rebecca Heald,‡ Kumiko Samejima,* William C. Earnshaw,* and Don W. Cleveland§

*ICMB, University of Edinburgh, Edinburgh EH9 3JR, Scotland; ‡Department of Molecular and Cell Biology, University of California Berkeley, Berkeley, California 94720; and §Ludwig Institute for Cancer Research and Division of Cellular and Molecular Medicine, University of California San Diego, La Jolla, California 92093-0660

Abstract. NuMA is a large nuclear protein whose relocation to the spindle poles is required for bipolar mitotic spindle assembly. We show here that this process depends on directed NuMA transport toward microtubule minus ends powered by cytoplasmic dynein and its activator dynactin. Upon nuclear envelope breakdown, large cytoplasmic aggregates of green fluorescent protein (GFP)-tagged NuMA stream poleward along spindle fibers in association with the actin-related protein 1 (Arp1) protein of the dynactin complex and cytoplasmic dynein. Immunoprecipitations and gel filtration demonstrate the assembly of a reversible, mitosis-specific complex of NuMA with dynein and dynactin. NuMA transport is required for spindle pole assembly and maintenance, since disruption of the dynactin complex (by increasing the amount of the dynamitin subunit) or dynein function (with an antibody) strongly inhibits NuMA translocation and accumulation and disrupts spindle pole assembly.

Key words: mitosis • microtubules • motor proteins • centrosome • spindle pole matrix

Introduction

The formation of bipolar mitotic spindles is a prerequisite to ensure the symmetrical distribution of chromosomes to each daughter cell. Spindles consist of two arrays of microtubules, anchored with their minus ends at the poles and their plus ends extending towards the equator, where they partially overlap in an antiparallel fashion. The spindle microtubules can provide both force and guidance for chromosome movement. Further, by converging towards the spindle poles, they concentrate chromosomes in two defined areas, where these are packed into daughter nuclei.

A variety of proteins that are involved in spindle morphogenesis have been characterized during the last few years. Essential proteins for pole formation include centrosomal components, such as γ-tubulin (Joshi et al., 1992; Stearns and Kirschner, 1994) and pericentrin (Doxsey et al., 1994), as well as proteins that are not directly anchored to the pericentriolar material, such as NuMA (Lydersen and Pettijohn, 1980), dynactin (Gaglio et al., 1996, 1997), several microtubule-dependent motor proteins, including dynein (Heald et al., 1996, 1997) and XKLP2 (Boleti et al., 1996), and the small GTPase, Ran (reviewed by Kahana and Cleveland, 1999).

Prior efforts have shown that NuMA, a nuclear protein that relocalizes to the spindle poles during mitosis and meiosis, is necessary to focus microtubules into spindle poles and to control the size of mitotic spindles (Merdes et al., 1996). It is enriched in a crescent-shaped area at the spindle poles, and EM demonstrates that the majority of the protein is located between microtubules (Dionne et al., 1999). Immunoprecipitation of NuMA from metaphase-arrested frog egg extracts further revealed an association of NuMA with cytoplasmic dynein and its activator complex dynactin. The mechanisms by which this complex is formed, how NuMA becomes pole-associated, and the precise role of this complex in linking spindle microtubules to each other or the centrosome have not been identified.

Several studies have shown that the formation of spindle poles is inhibited in the presence of a mAb against the dynein intermediate chain (Heald et al., 1996, 1997; Gaglio et al., 1997). At the same time, however, dynein motor activity seems unaffected by this treatment (Heald et al., 1997). The situation is further complicated by the fact that bundling of microtubules into a convergent polar array needs one or more components with multiple microtubule binding sites. Although the dynein motor possesses one such binding site on each subunit of the heavy chain dimer, these two sites are both needed for processive movement and, therefore, unlikely to be involved in tethering microtubule bundles. Rather, the known dynein dependency for

Address correspondence to Andreas Merdes, ICMB, University of Edinburgh, King's Buildings, Edinburgh EH9 3JR, Scotland, UK. Tel.: 011 44 131 650 7075. Fax: 011 44 131 650 7360. E-mail: a.merdes@ed.ac.uk

tethering spindle microtubules into poles must involve proteins with additional microtubule binding sites. Candidates for these include dynactin (Waterman-Storer et al., 1995) and NuMA (Merdes et al., 1996), both of which have been shown to bind to microtubules themselves.

From this background, we now use a combination of green fluorescent protein (GFP)[1]-tagging of NuMA in vivo, immunoprecipitation and gel filtration, and antibody disruption to identify the mechanism of formation of focused spindle poles.

Materials and Methods

Transfection Experiments and Microscopy

For the expression of GFP-tagged NuMA in tissue culture cells, a construct was assembled that contained full-length human NuMA (Compton et al., 1992). NuMA was modified at its 5′ end by PCR using a primer (GCAGGCGGCCGCATGACACTCCAC) that encoded a Not1 restriction site followed by the start codon. This site was used to join NuMA in frame to the 3′ end of GFP that was in turn modified by adding a Not1-containing hinge region of 42 bp (CCAGGAGCCGGCGCAGGTGCTGGAGCAGGTGCAGGCGGCCGC), eliminating the stop codon of GFP. The construct was inserted into the expression vector pcDNA3 (Invitrogen) using EcoR1 and Xba1 restriction sites. HeLa cells were grown on glass coverslips in DME containing 10% FBS (GIBCO BRL). Transient transfection experiments of GFP-NuMA were carried out using calcium phosphate precipitation, as described in Sambrook et al. (1989). The transfection efficiency was tested by immunoblotting, using the mAb 1F1 against human NuMA (Compton et al., 1991), and by counting GFP-positive cells under the fluorescence microscope. To assess the degree of GFP-NuMA overexpression in individual cells, immunofluorescence staining with the 1F1 antibody, recognizing both GFP-NuMA and endogenous NuMA, and a secondary Texas red-coupled anti-mouse antibody was performed. The intensity of the Texas red fluorescence in interphase nuclei of 23 randomly selected GFP-NuMA–expressing cells and 30 control cells was quantified from confocal microscope sections as pixel intensity per nuclear section area, after subtraction of the background fluorescence calculated from five different representative areas.

For time-lapse observations of GFP-NuMA, coverslips containing cells were mounted in growth medium onto microscope slides using a vaseline-coated rubber O-ring as spacer. Recordings of 0.5-s exposure time were made at 19°C in 2-min intervals using a Photometrics Sensys cooled CCD camera, containing a KAF1400-G2 chip. The camera was mounted on a Zeiss Axioskop, using a Plan-Apochromat 63×/1.40 lens, and a filterwheel/shutter device (American Precision 23D-6102A, control box LEP/LUDL), controlled by Quips Imaging Software (Vysis) on a PowerMacintosh 8600/200 computer (Apple). Alternatively, recordings at 37°C were made with the same equipment, and a temperature-controlled fan heater mounted next to the microscope stage.

Spindle Formation Assays and Immunofluorescence

For the formation of spindles in vitro, *Xenopus laevis* egg extract and *Xenopus* sperm were prepared and centrifuged onto glass coverslips as described in Merdes et al. (1996). Direct formation of spindles from frog sperm in cytostatic factor (CSF)-arrested extract was monitored for ~1 h. Dynein inhibition experiments were carried out by adding monoclonal dynein intermediate chain antibody 70.1 (Sigma Chemical Co.) dialyzed against PBS to the extract at the beginning of the incubation with frog sperm, at a final concentration of 0.1 mg/ml immunoglobulin. Dynactin was inhibited by the addition of dynamitin at a final concentration of 0.75 mg/ml. For this experiment, a dynamitin clone was obtained by PCR from a HeLa cDNA library (provided by S. Kandels-Lewis, University of Edinburgh, Scotland) using primers ATGGCGGACCCTAAATACGCC and TCTCACTTTCCCAGCTTCTTC. Sequencing revealed that a dynamitin isoform was cloned that lacked amino acids 36-40, but was otherwise identical to the previously published human dynamitin sequence (Echeverri et al., 1996). The dynamitin PCR product was cloned in the vector pCR-TM2.1, excised using EcoR1, and cloned into the bacterial expression vector pRSET A (both from Invitrogen). Bacterial fusion protein was isolated using 8M urea and dialyzed against PBS before the assay. NuMA was inhibited by adding antibodies against the distal *Xenopus* NuMA tail (Merdes et al., 1996) to preformed spindles for 10 min. Control spindles were assembled while adding equivalent volumes (up to 20% of the extract volume) of PBS.

HeLa cells were fixed for 10 min in methanol at −20°C. After rehydration and rinsing in PBS, cells were labeled with antibodies against human NuMA (clone 1F1, see Compton et al., 1991), *Xenopus* NuMA/distal tail domain (Merdes et al., 1996), actin-related protein 1 (Arp1)α/A27 (Clark and Meyer, 1999), dynein heavy chain (Heald et al., 1997), Eg5 (Sawin et al., 1992), α-tubulin, clone DM1A (Sigma Chemical Co.). Secondary antibodies, coupled to FITC or Texas red, were from Vector. Chromosomes were stained using 4′,6′-diamidino-2-phenylindole (DAPI; Sigma Chemical Co.), and coverslips were embedded in Vectashield (Vector). For conventional fluorescence microscopy, equipment was used as described above. For confocal microscopy, a Leica DM IRBE microscope with a PL APO 100×/1.4 lens was used; the device was equipped with argon, krypton, and UV lasers for excitation (at 488, 568, and 360 nm, respectively), and a Leica TCS SP multi band spectrophotometer for detection, controlled by Leica TCS NT software. Default settings for FITC, Texas red and DAPI were used.

The dependence of NuMA transport on intact microtubules was studied in GFP-NuMA–expressing and control cells. GFP-NuMA aggregates were visualized in living cells as described above. Cells were then exposed to nocodazole at 10 μg/ml in culture medium for 1 h. Subsequently, cells were either incubated with fresh culture medium for 45 min to remove the nocodazole or fixed directly, and stained for tubulin immunofluorescence. Cells were relocated on the microscope using the stage coordinates, as well as reference pictures taken with phase-contrast microscopy.

Immunoprecipitation of NuMA from Frog Egg Extracts

For the immunoprecipitation of NuMA, affinity beads were prepared by coupling periodate-treated goat anti–rabbit antibody (Jackson ImmunoResearch Laboratories) to Affi-Prep-Hz hydrazide support (BioRad), according to the manufacturer's instructions. These beads were then coated with antibody against the *Xenopus* NuMA distal tail region, and NuMA was removed from extracts as described (Merdes et al., 1996). After immunoprecipitation, beads were washed five times with 60 mM KCl, 15 mM NaCl, 15 mM Tris/HCl, pH 7.4, once with buffer containing 0.2% Triton X-100, and finally boiled for 5 min in gel loading buffer, containing SDS and mercaptoethanol. Coimmunoprecipitation of other proteins was tested by gel electrophoresis and immunoblotting, using antibodies against dynein heavy chain, dynein intermediate chain, Arp1, and Eg5 as described above, as well as antikatanin/p60 subunit (Hartman et al., 1998), and antidynactin p150/glued, mAb 150B (Quintyne et al., 1999). Inhibition of dynein or dynactin coprecipitation was performed using mAb 70.1 or dynamitin, as described above. Experiments in interphase frog egg extract were carried out by converting metaphase arrested egg extract by addition of 2 mM calcium chloride and incubation at room temperature for 45 min. The cell cycle state of the extract was monitored by testing 1-μl aliquots for histone H1 kinase activity exactly as described by Murray (1991). Subsequent NuMA immunoprecipitation was performed within 20 min, and aliquots of the immunoprecipitation supernatants of both interphase and metaphase extracts were tested again for kinase activity, to verify that these extracts had not proceeded in the cell cycle.

Gel Filtration Chromatography

A gel filtration column of 80-cm length was prepared using 200 ml Sepharose 4B (Sigma Chemical Co.) in 60 mM KCl, 15 mM NaCl, 15 mM Tris/HCl, pH 7.4, 1 mM β-mercaptoethanol, and 0.1 mM PMSF. The flow rate was 0.14 ml/min. The column was calibrated using blue dextran (2,000 kD), thyroglobulin (669 kD), ferritin (440 kD), catalase (232 kD), and aldolase (158 kD) as markers. CSF-arrested frog egg extract was cleared by centrifugation at 18,000 *g* for 15 min. 100 μl of extract was loaded onto the column. Fractions of 4-ml size were precipitated with 10% trichloroacetic acid, washed with acetone, and analyzed by gel electrophoresis and immunoblotting. The migration position of tubulin dimers (110 kD) was determined by immunoblotting and used as an internal size standard. A different gel filtration column of 45-cm length was prepared with 30 ml Sephacryl S-400 (Sigma Chemical Co.) in the same buffer as above. 50 μl

[1]*Abbreviations used in this paper:* Arp1, actin-related protein 1; CSF, cytostatic factor; DAPI, 4′,6′-diamidino-2-phenylindole; GFP, green fluorescent protein.

of extract was loaded, and fractions of 1-ml size were collected and treated as above.

Microtubule Seed Transport Assay

Spindles were assembled around DNA-coated magnetic beads in control and NuMA-depleted frog egg extracts, cycled from interphase into mitosis (Heald et al., 1996, 1997). NuMA depletion was performed as described (Merdes et al., 1996). Rhodamine-labeled seeds were prepared and video microscopy was performed as described (Heald et al., 1996, 1997).

Results

NuMA Colocalizes with Dynactin after Nuclear Envelope Breakdown

To determine how NuMA is transported after nuclear envelope disassembly, NuMA location was identified in cells just transitioning from prophase to prometaphase. As described previously (Compton et al., 1992; Yang et al., 1992), NuMA was found almost homogeneously distributed in the nucleoplasm during interphase (not shown). However, during prophase, while chromosome condensation took place, the localization of NuMA was restricted to the interchromatin space. Fig. 1 A shows a typical conventional immunofluorescence picture of a late prophase, in which NuMA was found in those areas of the nucleus that were not occupied by the condensed chromosomes (for comparison, see also Compton et al., 1992; Yang et al., 1992). At this stage, the actin-related protein Arp1, a subunit of the motor–cargo-mediating complex dynactin, decorated the duplicated centrosomes and astral microtubules radiating from them (Fig. 1 B). With the transition to prometaphase (identified by the absence of the round contour of the nuclear envelope), small aggregates of NuMA were grouped in radial arrays colocalizing with astral Arp1 (Fig. 1, C and D).

In many prometaphase cells, besides the material that had already accumulated at the poles, larger aggregates of NuMA (Fig. 1 E) in association with Arp1 (Fig. 1 F) were found approximately in the midzone of the spindle. The occurrence of nonpolar NuMA-containing aggregates was found in cells from various species, including HeLa cells, *Xenopus* A6 cells (Fig. 1, I and J) and chicken DU249 cells (not shown). The staining of these aggregates was detected with three different antibodies: mAb 1F1 against human

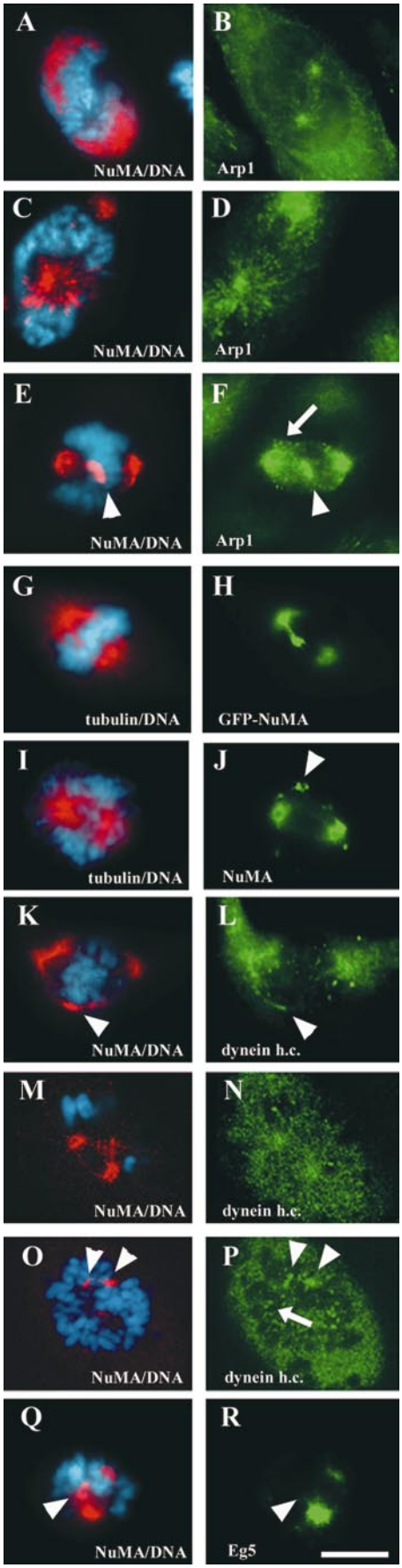

Figure 1. NuMA, dynactin, and dynein are present in aggregates in early prometaphase spindles. A–H and K–R, HeLa cells (A and B) in prophase. C–H and K–R, HeLa cells in early stages of prometaphase. I and J, A *Xenopus* A6 cell in early prometaphase. A, C, E, J, K, M, O, and Q, Endogenous NuMA (red) is detected by immunofluorescence or (H) transfected GFP-NuMA is shown. In B, D, and F, the dynactin subunit Arp1 is stained. L, N, and P, Cytoplasmic dynein heavy chain is shown. M and N, and O and P, are pairs of confocal sections, at the level of the spindle poles and at the bottom of the cell, respectively. G and I, Depict tubulin immunofluorescence. R, Displays the localization of the kinesin-related motor, Eg5. Chromosomes are stained with DAPI and displayed in blue in these panels. Arrows in F and P indicate kinetochore staining of Arp1 and dynein, respectively, whereas arrowheads in E, F, J, K, L, O, P, Q, and R mark the positions of NuMA aggregates outside the poles. Bar, 20 μm.

NuMA (Compton et al., 1991), polyclonal anti-*Xenopus* NuMA tail (Merdes et al., 1996), and a newly generated mAb against chicken NuMA (Merdes, A., unpublished observation). The shape and size of these aggregates varied from cell to cell, but nonpolar NuMA aggregates were found in 64% of prometaphases ($n = 244$) of HeLa cell cultures. It appeared that these aggregates were mainly found in early stages of prometaphase, but were absent after a bipolar spindle apparatus had fully formed, and after the majority of the chromosomes had been bi-oriented. Many NuMA aggregates were found in focal planes different from the spindle poles, which may explain why they have not been documented in previous reports. As shown in Fig. 1, G and H, this aggregated NuMA frequently stretched along spindle fibers towards the spindle poles, suggesting that NuMA was under a microtubule-dependent pulling force.

Because the kinesin-related microtubule motor Eg5 has been shown to participate in spindle pole organization (Gaglio et al., 1996) and because Eg5 was also reported to bind to the dynactin complex (Blangy et al., 1997), we wanted to test for potential localization of Eg5 on NuMA aggregates. Although Eg5 was enriched at developing spindle poles in prometaphase cells, it was not enriched on the NuMA aggregates outside the pole regions (Fig. 1, Q and R). Cytoplasmic dynein, on the other hand, partially colocalized in prometaphase cells with NuMA aggregates (Fig. 1, K and L, arrowhead). This colocalization was confirmed using the three-dimensional resolution of a confocal microscope, equipped with a spectrophotometer for detection to exclude bleed-through of NuMA fluorescence onto the dynein signal (Fig. 1, M–P). In addition to dynein associated with NuMA, the bulk of dynein was found more diffusely within the cytoplasm (Fig. 1, L, N, and P) or at kinetochores (Fig. 1 P, arrow), as also seen for the dynactin subunit, Arp1 (Fig. 1 F). This suggests that only a proportion of the pool of dynein and dynactin attaches to NuMA aggregates, to pull these towards the poles.

Poleward Transport of GFP-tagged NuMA in Living Cells

To test the idea of dynein/dynactin-dependent NuMA transport to the spindle poles in living HeLa cells, we expressed full-length NuMA tagged at its extreme NH_2 terminus with GFP. This GFP-NuMA showed a cell cycle-dependent relocalization from the interphase nucleus to the spindle poles that was indistinguishable from endogenous NuMA (Fig. 2, A–D). Cells expressing GFP-NuMA were observed at all stages of the cycle with no apparent consequences arising from accumulation of the chimeric NuMA. To determine the levels of GFP-NuMA overexpression, we performed immunoblotting of transiently transfected HeLa cell cultures using an antibody that recognizes both GFP-NuMA and endogenous NuMA. Besides the 240-kD band of endogenous human NuMA, the transfected cells revealed an additional band representing GFP-tagged NuMA (Fig. 2 E, right lane). By fluorescence microscopy we counted that ~12% of the cells (252 in 2,035) were overexpressing GFP-NuMA in a typical experiment. The level of overexpression in individual cells, as measured by quantitative immunofluorescence microscopy (see Materials and Methods), ranged from 1.2- to 3.8-fold, with an average level of 2.2-fold of the endogenous NuMA level ($n = 23$ for GFP-NuMA expressors, $n = 30$ for controls). GFP-tagged NuMA accumulated in nonpolar aggregates during early stages of prometaphase (Fig. 2 F) in the same way as endogenous NuMA stained with antibodies (Fig. 1). In combination, these observations ruled out the possibility of an artifact due to overexpression, or vice versa, a staining artifact of our antibodies.

Time-lapse recordings of GFP-NuMA revealed that the midzone aggregates were stretched towards both spindle poles (Fig. 2 F, 5–13 min) and then moved towards the poles along tracks of spindle fibers (Fig. 2 F, 13–37 min). Whereas some of the initial movements seemed to occur along few defined tracks (between 13 and 21 min), later stages showed NuMA transport across the entire half spindles (for example, see diffuse GFP-NuMA signal in the upper half spindle at 37 min in Fig. 2 F). This might simply reflect the fact that the density of spindle microtubules is lower early in prometaphase (Roos, 1973). Between 37 and 63 min, nearly all GFP-NuMA had accumulated at the spindle poles. Small cytoplasmic aggregates of GFP-NuMA were also visible in some fields (Fig. 2 G, arrow), being pulled towards the spindle poles at an average speed of 1 μm/min ($\pm$ 0.3, $n = 3$) when these experiments were carried out at 19°C. When the microscopy was performed at 37°C instead, movements ranging from 1.7–4.5 μm/min were measured, yielding an average speed of 2.6 μm/min ($\pm$ 1.0, $n = 8$). These transport velocities are in good agreement with rates for dynein-dependent movement of microtubule seeds measured in spindles, which yielded a median speed of ~2.5 μm/min, with several very rapid movements producing an average of 6 μm/min (Heald et al., 1997).

To examine the dependence of poleward NuMA transport on the integrity of spindle microtubules, we subjected prometaphase cells to treatment with nocodazole (Fig. 2 H). After incubation with nocodazole, all microtubules had been dissolved (Fig. 2 H, right). At the same time, all pole-accumulated NuMA, as well as nonpolar NuMA aggregates that were visible initially in the untreated cell (Fig. 2 H, left) were completely solubilized (Fig. 2 H, middle). When nocodazole-treated cells were allowed to recover in fresh culture medium, the spindle apparatus reformed (Fig. 2 I, left), and NuMA accumulated at the poles again (Fig. 2 I, right). Besides, new aggregates of NuMA formed in the cytoplasm and along the spindle apparatus (Fig. 2 I, right).

NuMA Associates with Dynactin and Dynein in a Low-affinity Complex

Our data on minus end-directed GFP-NuMA transport suggest that cytoplasmic dynein is the driving force for NuMA accumulation at the poles, in agreement with our previous findings showing that a complex of dynein, dynactin, and NuMA can be immunoprecipitated from metaphase-arrested frog egg extracts (Merdes et al., 1996). To examine further the composition and properties of this complex, immunoblots of anti-NuMA immunoprecipitates from metaphase egg extracts were examined with the repertoire of available antibodies that react with frog dynein/dynactin

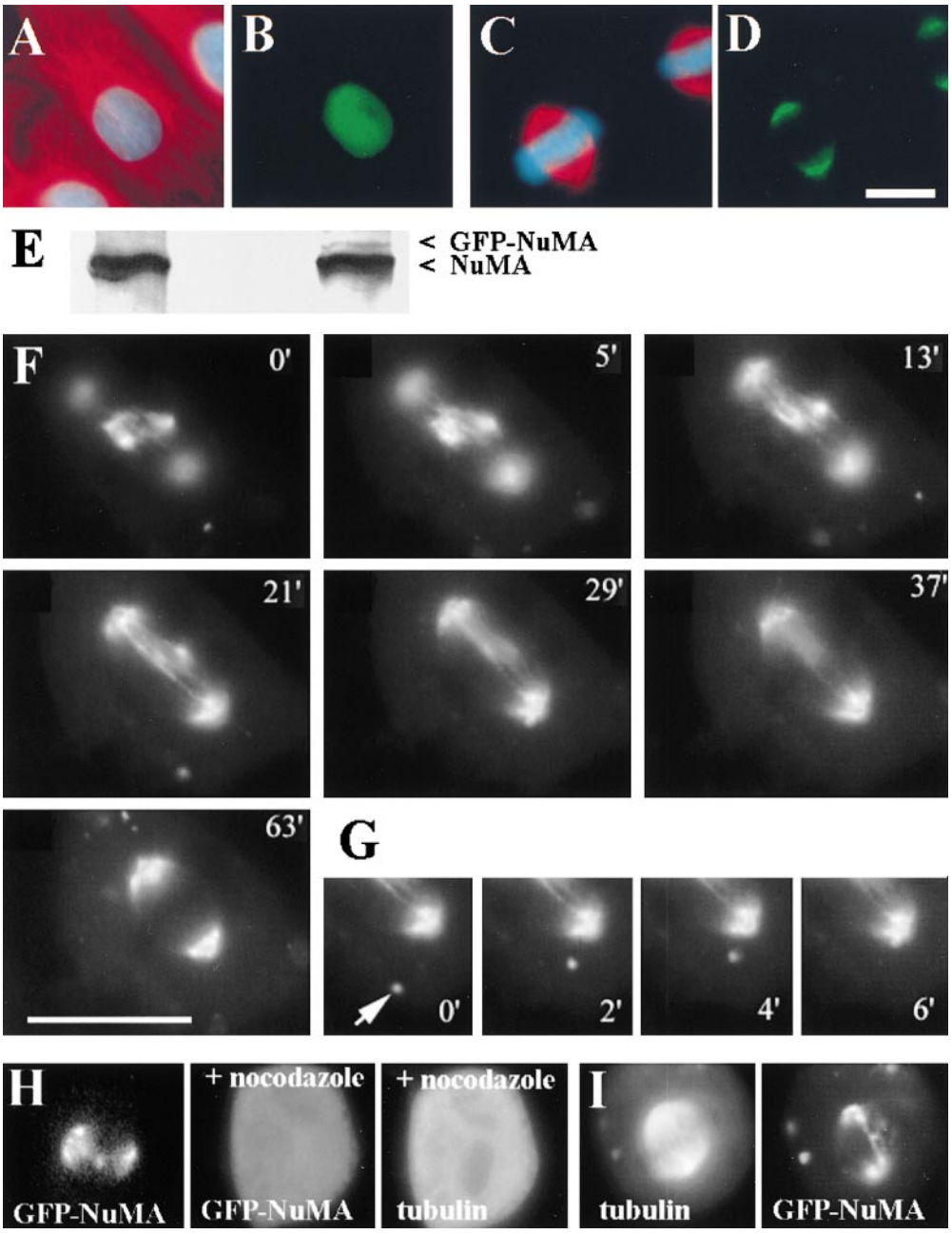

Figure 2. GFP-NuMA is transported towards the poles along spindle fibers. A–D, Correct cell cycle-dependent localization of overexpressed GFP-NuMA in HeLa cells. A, An interphase HeLa cell is stained for tubulin (red) and DNA (blue). B, GFP-tagged NuMA (green) localizes to the nucleus of the same cell. C and D, Two metaphase cells, stained for tubulin (red) and DNA (blue), show localization of GFP-NuMA (green) at the spindle poles. E, Immunoblot of NuMA in cultures of control cells (left lane), and GFP-NuMA–expressing cells (right lane). An additional band of higher molecular weight, representing GFP-tagged NuMA, is visible in the right lane. F, Selected phases of a time-lapse series of GFP-NuMA in a HeLa cell in prometaphase. G, A small NuMA-containing particle is transported from the periphery of the cell towards the mitotic spindle pole. H (left), A living prometaphase cell overexpressing GFP-NuMA is shown. Besides GFP-NuMA at the poles, a nonpolar NuMA aggregate in the spindle midzone is visible. The same cell after nocodazole treatment, followed by fixation and tubulin immunofluorescence (right). Note that all GFP-NuMA is solubilized (middle). I, A different cell, after repolymerization of microtubules (left), after nocodazole treatment. New GFP-NuMA aggregates have formed, and a fraction of NuMA has accumulated at the spindle poles. Bars, 20 μm. G is at the same magnification as F.

components. This revealed that dynein heavy and intermediate chains, as well as dynactin p150 and the actin-related protein Arp1, were complexed with NuMA (Fig. 3 A). The pole-enriched microtubule-severing factor, katanin (McNally et al., 1996), or the kinesin-related motor, Eg5, did not coimmunoprecipitate with NuMA (Fig. 3 A), underlining the specificity of these coimmunoprecipitation results. Further, the association of NuMA with dynein and dynactin is cell cycle dependent: when NuMA was immunoprecipitated from frog egg extracts released from metaphase arrest, the level of both coimmunoprecipitated dynactin and dynein was significantly reduced (Fig. 3 B).

To dissect the associations within this complex, the effects of inhibitors disrupting dynein and dynactin were examined. Coprecipitation was significantly reduced by each of two different inhibitors. First, the 50-kD dynactin subunit dynamitin, a well characterized inhibitor known to disrupt the integrity of the dynactin complex (Echeverri et al., 1996; Quintyne et al., 1999), abolished coimmunoprecipitation of dynactin subunits with NuMA. Further, probably as a consequence of dynactin disassembly, this also inhibited coprecipitation of dynein. Thus, dynein binding to NuMA apparently requires an intact dynactin complex as adaptor. Second, coimmunoprecipitation of both dynein

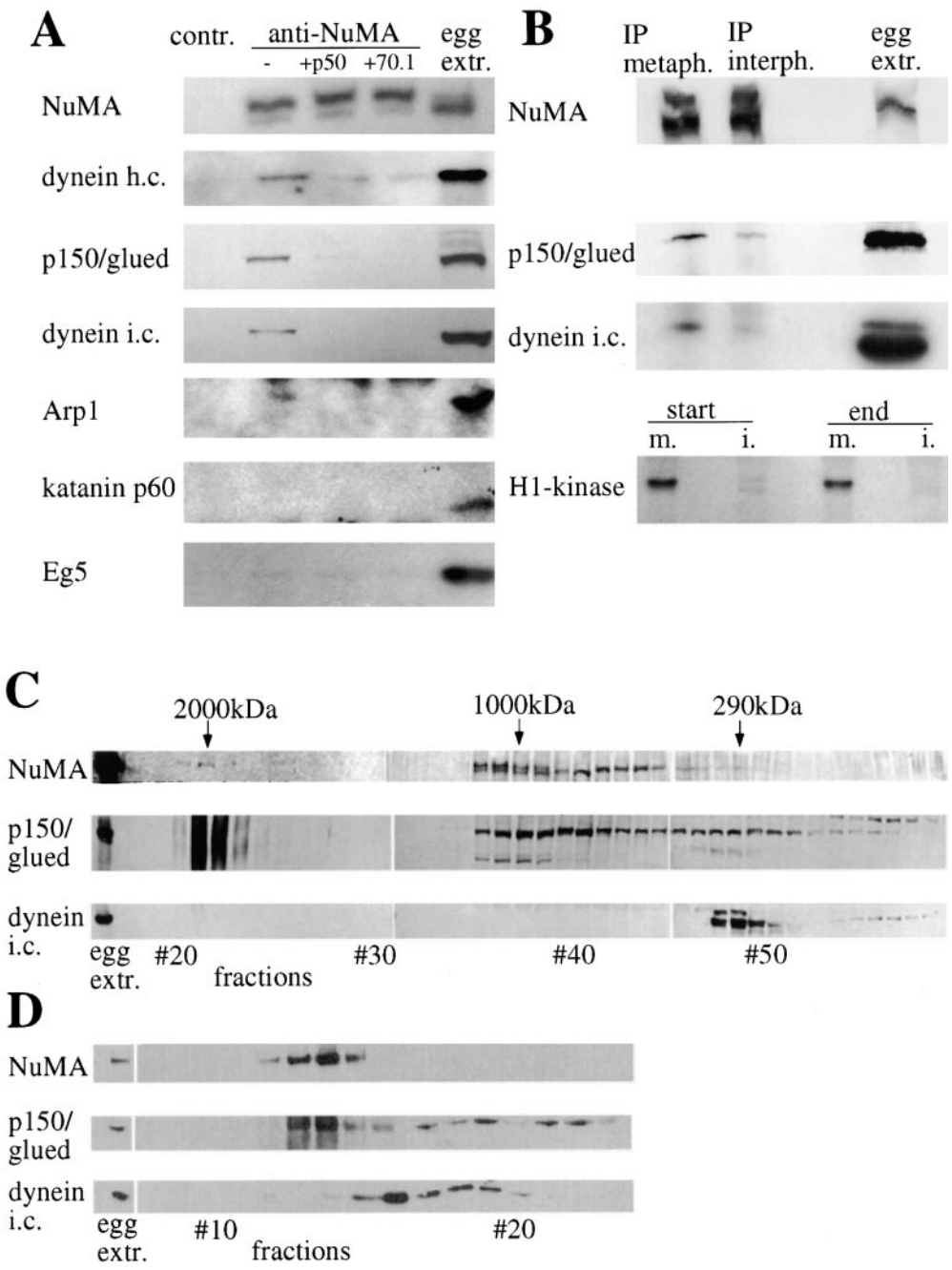

Figure 3. A complex of NuMA, dynactin, and dynein is present in metaphase egg extracts. A, Immunoprecipitation experiments using a rabbit antibody against a COOH-terminal region of the *Xenopus* NuMA tail, or a control preimmune serum. Regular precipitations are shown in the first two columns, the following columns show experiments to which inhibiting amounts of dynamitin or antidynein intermediate chain mAb 70.1 were added. The last column displays immunoblots of 1 μl amounts of *Xenopus* egg extract. In the different rows, immunoblots are shown of *Xenopus* NuMA, cytoplasmic dynein heavy chain, dynactin p150/glued, cytoplasmic dynein intermediate chain, dynactin Arp1α, katanin p60, and Eg5. Dark bands appearing at the top of the Arp1 immunoblot and at the bottom of the katanin immunoblot represent staining of the precipitating rabbit IgG at ~50 kD by ^{125}I-protein A. B, The coimmunoprecipitation of dynactin and dynein is mitosis-specific. Immunoblots of NuMA precipitations and frog egg extract aliquots were probed with antibodies against NuMA, dynactin p150/glued, and dynein intermediate chain. Metaphase-arrested extract and interphase extract were used for immunoprecipitations. Bottom, Autoradiography of phosphorylated histone H1 in mitotic (m.) and interphase (i.) extracts. Aliquots before and after completion of the immunoprecipitation were tested. C, Fractions of frog egg extract after a Sepharose 4B gel filtration column, tested by immunoblotting for NuMA, dynactin p150/glued, and dynein intermediate chain. Aliquots of extract before column chromatography are shown on the left. Molecular weight positions calculated from the calibration standards are indicated on the top. D, Column fractions from a Sephacryl S-400 gel filtration column of shorter size and shorter running time, immunoblotted for NuMA, dynactin p150/glued, and dynein intermediate chain.

and dynactin components was strongly inhibited by mAb 70.1 against dynein intermediate chain. As discussed by Gaglio et al. (1997), this antibody does not only affect the function of dynein itself in HeLa cell extracts. It does, however, apparently solubilize dynactin subunits from larger microtubule aster assemblies, thereby implicating a cooperative interaction between the dynein intermediate chain and its dynactin binding partner, p150/glued, as essential to the stabilization of a larger microtubule-binding complex that is disrupted by the mAb (Gaglio et al., 1997). Release of dynactin from NuMA by mAb 70.1 (Fig. 3 A) thus indicates that NuMA must also be a part of this larger complex.

To determine the size and stability properties of the cytoplasmic dynein and dynactin associated with NuMA, mitotic frog egg extracts were fractionated over a Sepharose 4B gel filtration column. This revealed a small amount of both dynactin p150 and NuMA coeluting with the size

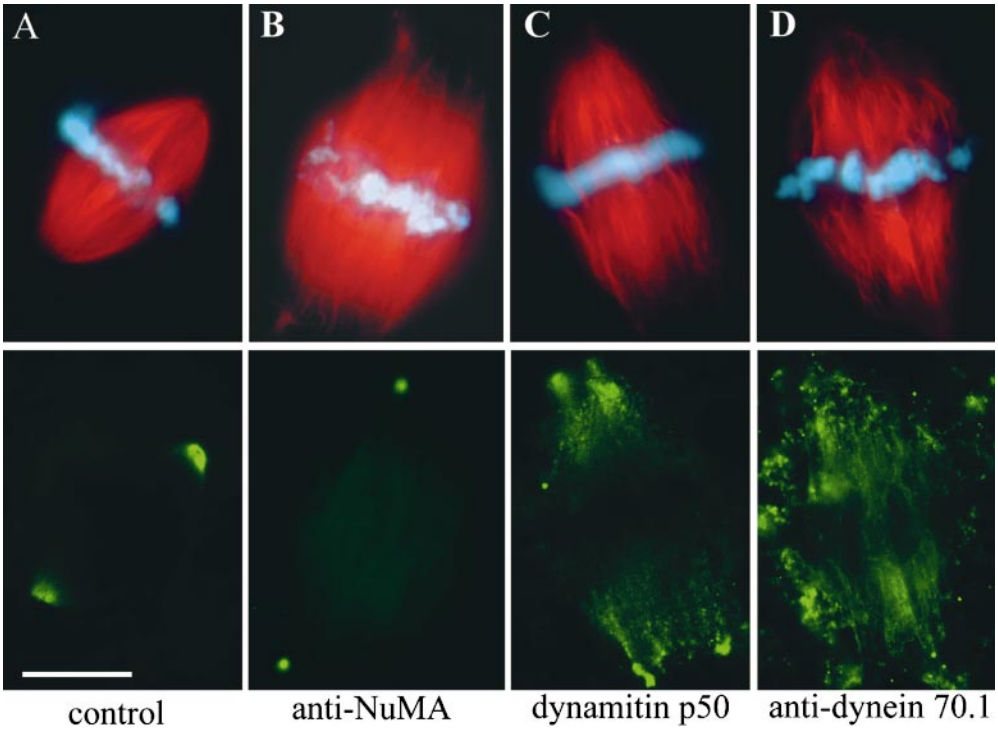

Figure 4. Dynein and dynactin inhibitors interfere with NuMA transport and spindle pole formation. Spindles assembled around frog sperm chromatin in CSF-arrested egg extracts. A, Control spindle; B, spindle treated with anti-NuMA antibody; C, spindle assembly inhibited by dynamitin; D, spindle assembly inhibited by antibody against dynein intermediate chain. Top, rhodamine-labeled tubulin (red), and DNA (blue). Bottom: A, C, and D, NuMA immunofluorescence; or B, localization of anti-NuMA by secondary antibody. Bar, 20 μm.

marker dextran, consistent with a complex of 2,000 kD or higher (Fig. 3 C). The dynactin p150 always appeared as an unfocused band in these fractions, suggestive of an as yet unidentified covalent modification. The majority of NuMA and dynactin, however, was detected in fractions of an intermediate size, at ~1,000 kD, whereas the bulk of the dynein intermediate chain eluted at a much later position (corresponding to ~290 kD). Dynein heavy chains were found at ~800 kD and did not copurify with the intermediate chains (data not shown). This indicated that most components of the basic dynein motor complex (consisting of at least two heavy chains of 400–500 kD, two intermediate chains of 70 kD, and several light chains and a native molecular weight expected to exceed 1,000 kD) had disassembled during chromatography. This reinforces the immunoprecipitation findings that NuMA, dynactin, and dynein form a low-affinity complex that is easily disassembled by dilution. Moreover, they also demonstrate that the weakest or most transient interaction is of NuMA with the dynein motor component itself.

To test whether smaller dilutions and/or shorter chromatography times would preserve higher amounts of cofractionating NuMA and dynactin, similar extracts were fractionated on a sephadex S-400 column of only 45-cm length. Under these conditions, dynein again eluted in fractions distinct from NuMA and dynactin. However, almost all NuMA chromatographed with a proportion of dynactin p150, which again displayed a diffuse electrophoretic mobility selectively in the NuMA-containing fractions (Fig. 3 D). Further evidence for the transient and reversible nature of the NuMA complexes with dynactin and dynein was obtained by sedimentation analysis on 10–40% sucrose gradients (not shown). This revealed that associations between NuMA and dynactin or dynein were completely lost during the long times required for sedimentation, with NuMA sedimenting in two peaks of 8S and 35S. The bulk of dynein heavy chain and dynactin components sedimented at 20S, as reported previously (Schroer and Sheetz, 1991).

Disruption of Dynactin or Dynein Inhibits NuMA Transport and the Formation of Spindle Poles

To directly test whether NuMA is transported towards the spindle poles by association with dynein and dynactin, spindles assembled in metaphase-arrested frog egg extracts were monitored for the effects of dynein and dynactin inhibitors. Control extracts yielded regularly shaped spindles ~60 min after addition of frog sperm DNA (Fig. 4 A).

Even preformed spindles were sensitive to treatment with antibodies against NuMA, which provoked the release of the centrosomes from the spindles and the splaying of microtubule ends previously focused to form each pole (Fig. 4 B). Serial sectioning and EM confirmed that the disconnected small microtubule asters (with anti-NuMA staining in their core) indeed contained centrosomes (not shown). Addition of high levels of the dynactin inhibitor dynamitin during the process of spindle formation produced a very similar phenotype of unfocused poles (Fig. 4 C). In this case, NuMA was no longer restricted to the microtubule minus ends, but seen along the entire length of the spindle fibers (Fig. 4 C, bottom). Consistent with earlier observations (Heald et al., 1997; Gaglio et al., 1997), an almost identical effect was seen by addition of the dynein intermediate chain antibody 70.1 (Fig. 4 D). These data indicate that there is a direct dependence of NuMA accumulation at the poles on dynein/dynactin-mediated transport. It should be noted that a certain amount of NuMA is nevertheless seen at microtubule minus ends, de-

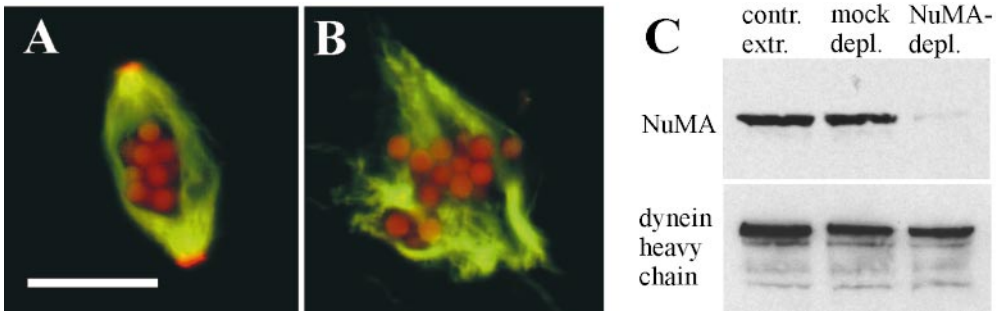

Figure 5. Microtubule seeds are transported towards the poles in a NuMA-dependent mechanism. A and B, Spindles assembled around DNA-coated magnetic beads in frog egg extract cycled from interphase into mitosis. Green, FITC-labeled tubulin; red, rhodamine-labeled microtubule seeds. (In addition, the magnetic beads used in this assay show a substantial amount of red autofluorescence.) A, Control spindle. B, Aberrant spindle assembled in NuMA-depleted extract. C, Immunoblots of untreated control extract, mock-depleted extract with a control antibody, and extract after NuMA depletion probed with anti-NuMA antibody (top) or antidynein heavy chain (bottom). Bar, 20 μm.

spite dynein or dynactin inhibition. This partly could be due to NuMA's direct binding affinity to microtubules (Merdes et al., 1996), and an inherent microtubule translocation mechanism of the spindle, termed poleward flux (Mitchison, 1989). The disruption of dynactin and dynein in our experiments did, however, result in a dramatic disruption of the spindle poles, adding further weight to the model in which cohesion of microtubules at poles depends on the interaction between NuMA, dynein, and dynactin.

NuMA-dependent Tethering and Focusing of Polar Microtubules

Experiments in *Xenopus* egg extracts using rhodamine-labeled microtubule seeds previously have been used to show that focusing of poles may involve cytoplasmic dynein-mediated, minus end-directed sliding of microtubules along each other (Heald et al., 1997). In this model, stationary microtubules would provide the tracks, along which motile microtubules would be transported by dynein as a cargo. To analyze whether NuMA played any role in this microtubule movement, spindles in frog egg extracts were assembled around DNA-coated magnetic beads. These spindles were incubated with small microtubule seeds that were brightly labeled at their minus ends with rhodamine–tubulin. In control spindles, these microtubule seeds accumulated at the poles, on the minus ends of spindle fibers (Fig. 5 A). When we attempted to form spindles in extracts from which NuMA had been depleted with immobilized NuMA antibodies, only aberrant structures, lacking microtubules focused into poles were assembled around the DNA beads (Fig. 5 B). These structures were almost identical to spindles assembled in NuMA-free extracts around sperm chromatin (Merdes et al., 1996), or those formed in the presence of inhibitors, as shown in Fig. 4. Thus, NuMA is necessary for pole formation in spindle assembly either in the presence or absence of centrosomes. Moreover, virtually no microtubule seeds attached to these structures (Fig. 5 B). Thus, in these mitotic extracts NuMA is also necessary either for transport of microtubules relative to each other or for stabilizing the tethering of those microtubules after transit to the microtubule minus ends, or both. These effects are due to loss of NuMA, rather than depletion of dynein, since immunoblotting revealed that dynein was still present in abundance in these samples after nearly complete NuMA removal (Fig. 5 C), consistent with our earlier report that dynein is ~30 times more abundant than NuMA in these extracts (Merdes et al., 1996).

Discussion

The Role of NuMA, Dynein, and Dynactin at the Spindle Poles

We have for the first time observed the centripetal trafficking of NuMA to the poles during prometaphase. We have demonstrated that NuMA is transported along the mitotic spindle by the minus end-directed motor cytoplasmic dynein, in a complex with the activator dynactin. Further, we show that NuMA transport to the poles is necessary to form and stabilize the spindle and the spindle poles. Previously it was reported that dynein can drive the movement of microtubules within the spindle, with their minus ends leading towards the poles (Heald et al., 1996, 1997). From these studies and from work by others, a role of dynein and dynactin in the focusing of polar microtubule arrays was inferred (Gaglio et al., 1996, 1997; Echeverri et al., 1996). We now extend these observations by demonstrating that only a fraction of cytoplasmic dynein that associates with both dynactin and NuMA contributes to the formation of the spindle poles. In fact, the dynein-dependent accumulation of microtubule ends at the poles is only possible in the presence of NuMA, suggesting that NuMA is a critical factor involved in binding microtubules to each other.

We have shown previously that a region in the NuMA tail domain can bind microtubules and induce the formation of parallel microtubule bundles in vitro (Merdes et al., 1996). Therefore, in association with dynein and dynactin, NuMA can provide the necessary link that is required to attach a motile microtubule to the surface of a stationary microtubule, along which the dynein motor can glide (see model in Fig. 6, bottom). Alternatively, NuMA could reside on the surface of a stationary microtubule (Fig. 6, top) and the force production of the attached dynein motor could then be used to counterbalance outward-oriented forces of spindle-associated plus end-directed motors (Gaglio et al., 1996), thereby controlling the size of the spindle. This model is supported by our earlier finding that aberrant spindles assembled in NuMA-depleted frog egg

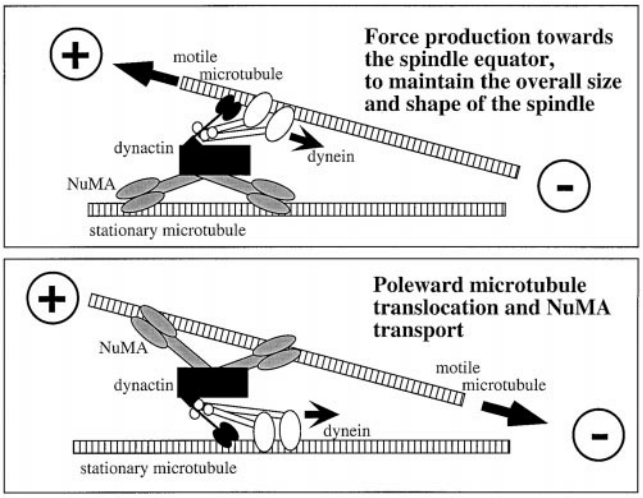

Figure 6. Model for NuMA/dynactin/dynein-dependent microtubule transport and focusing at the mitotic spindle. Top, NuMA (gray) can bind directly to a stationary microtubule and anchor other microtubules at the spindle pole through the dynactin complex (black) and the attached dynein motor (white). Thereby, dynein can provide inward oriented force at the spindle pole, maintaining the overall size of the spindle by counterbalancing outward-oriented forces from plus end-directed motors. Bottom, In reverse, NuMA can support microtubule transport towards the pole as part of the cargo-binding complex of the dynein motor by anchoring motile microtubules.

extracts are on average 1.5 times longer than control spindles. During the process of spindle formation, complexes of NuMA and dynein/dynactin could act as molecular ratchets that control the position of microtubules. In particular, this mechanism could help to stabilize parallel arrays of kinetochore fibers by preventing their minus ends from splaying apart, and thereby ensuring that linear tracks for anaphase chromosome separation are formed.

NuMA can assemble into oligomeric structures that are part of an insoluble, fibrous matrix. Indeed, recent EM work revealed the existence of NuMA in small electron-dense material located between spindle pole microtubules (Dionne et al., 1999). This, and the recent documentation of 12-arm NuMA oligomers formed in vitro or by overexpression of NuMA (Harborth et al., 1999), supports the idea that NuMA is a multivalent tethering factor that stabilizes the spindle poles independent of the centrosomes. Other than NuMA, spindle pole factors with similar functions are found in nonvertebrate organisms. For example, the recently characterized protein Asp in *Drosophila melanogaster* (Avides and Glover, 1999) localizes to the poles and possesses microtubule-binding capacity, and Asp-mutants in flies display an aberrant spindle morphology similar to that observed after inhibition of NuMA, dynein, or dynactin.

The Formation and Molecular Composition of the NuMA/Dynein/Dynactin Complex

In somatic cells, the interaction between NuMA and dynein/dynactin is restricted to mitosis, because during interphase NuMA is segregated to the nucleus, and spatially separated from cytoplasmic dynein and dynactin by the nuclear membrane. This compartmentalization does not exist in frog egg cytoplasm, where the majority of NuMA, dynein, and dynactin remains soluble during mitosis as well as during interphase. Nevertheless, the binding of NuMA to dynein and dynactin is mitosis-specific even in this system, as demonstrated in our coprecipitation experiments from metaphase and interphase frog egg extracts. This indicates that the interaction between NuMA, dynein, and dynactin must be specifically regulated. Our experiments both in frog egg extract and in mitotic HeLa cells demonstrate that the transport and pole accumulation of NuMA is a gradual process. Aggregates of NuMA are found in as many as 64% of HeLa cells in prometaphase, of which the majority is attached to the mitotic spindle. The formation of these aggregates could be explained in two different ways: one possibility is that they represent remnants of a NuMA meshwork that has formed as part of an insoluble nuclear matrix during interphase and that has not yet completely dissolved at the time of nuclear envelope breakdown, when the mitotic spindle is formed. In support of this would be the observation of NuMA meshworks that persist as late as prophase, filling the intranuclear space between the condensed chromosomes (Fig. 1 A; as well as Compton et al., 1992; Yang et al., 1992). Another possibility would be that all NuMA solubilizes at the prophase/prometaphase transition, but that the presence of spindle microtubules leads to condensation of soluble NuMA on their surface, if it cannot be transported to the spindle poles fast enough. This latter model would explain why NuMA aggregates are reversibly solubilized by the depolymerization of microtubules with nocodazole, but reform when microtubules are allowed to repolymerize. NuMA could thereby either bind directly to tubulin, as suggested before (Merdes et al., 1996), or bind to a different matrix formed in part by dynactin components. In any case, it appears that the poleward transport along spindle fibers is a rate-limiting step in dissolving these aggregates under physiological conditions.

Our microscopy data leave open the question whether NuMA is completely solubilized into homodimers (Harborth et al., 1995), or whether 12-arm oligomers, as recently described (Harborth et al., 1999), are transported along the spindle. What mechanisms promote disassembly of the interphase NuMA lattice or its mitosis-specific association with dynactin and dynein remains unknown, although it seems likely to involve posttranslational modification of NuMA: NuMA is phosphorylated at the G2/M transition (Sparks et al., 1995), and this phosphorylation seems to solubilize, at least in part, the fibrous meshwork residing in the nucleus during interphase (Saredi et al., 1997; Gueth-Hallonet et al., 1998; Harborth et al., 1999).

Our biochemical evidence makes it most likely that several NuMA dimers bind to dynactin to form a metastable complex, and recruit the dynein motor in a low-affinity interaction. This would explain why we can cofractionate NuMA and dynactin, but not dynein in our gel filtration experiments of metaphase-arrested frog egg extracts. The molecular size of our NuMA/dynactin fractions at ~2,000 kD would be consistent with the association of two dimers of NuMA (4×240 kD = 960 kD) with a dynactin complex

of ~1,200 kD, comprising ten subunits of Arp1, five subunits of p50/dynamitin, two subunits of p150/glued, and one subunit each of p62, p37, p32, p27, and p24 (Schafer et al., 1994). Consistently, after gel filtration, much of this complex is found disassembled, leaving both NuMA and dynactin at peaks of ~1,000 kD. After initial dynactin binding to NuMA, dynein could then attach transiently to this complex by an interaction between the dynein intermediate chain and the p150/glued subunit (Karki and Holzbaur, 1995; Vaughan and Vallee, 1995). As noticed by Schroer and Sheetz (1991), this interaction is not stable, a fact that is also reflected in the present study. The interaction of dynein with dynactin and NuMA, although detected by coimmunoprecipitation, is lost during the process of gel filtration. This might be due to the dilution in buffer and the long running times of our gel filtration columns (several hours), as compared with the immunoprecipitation protocol, in which washing is completed within a few minutes only. Further reflecting the transient nature of this interaction is the finding that dynein colocalizes only partially in some NuMA/dynactin midzone aggregates. Evidence for binding of NuMA to dynactin has also emerged from the findings of Clark and Meyer (1999), who showed that NuMA colocalizes to overexpressed wild-type Arp1α, but not mutant forms of Arp1α, even though these could still recruit other dynactin and dynein subunits. The binding of NuMA to dynactin was only seen in the cytoplasm of prometaphase cells in their experiments, but no longer during anaphase, indicating that the mitosis-specific binding between NuMA, dynactin, and dynein could be released as early as metaphase. Our in vivo observations add further support to this, revealing that all NuMA has been transported towards the poles at this stage, and might have been deposited to form an insoluble spindle pole matrix. An interaction between NuMA and the Arp1 filament of the dynactin complex thus seems likely, analogous to the suggested binding between Arp1 and Golgi apparatus-specific spectrin (Holleran et al., 1996).

Another factor that may be involved in the formation of this complex is an isoform of protein 4.1 (Mattagajasingh et al., 1999). Protein 4.1 binds directly to a region of the NuMA tail, both during interphase and mitosis. As suggested by Clark and Meyer (1999), 4.1 could mediate the binding of NuMA to Arp1, reflecting a similar binding hierarchy as on the erythrocyte membrane skeleton, where 4.1 interacts with spectrin and actin. Further work will be needed to define the specific role of protein 4.1 at the spindle poles.

We would like to thank Drs. T.A. Schroer (Johns Hopkins University), I.B. Clark, D. Meyer (UCLA), T. Mitchison (Harvard University), and F. McNally (UC Davis) for the donation of antibodies against dynactin p150, Arp1, Eg5, and katanin, respectively. We thank Dr. I. Stancheva (University of Edinburgh) for providing frog eggs, and the members of our laboratories for technical help and fruitful discussions.

This work was supported in part by a Wellcome Senior Research Fellowship to A. Merdes, a Wellcome Principal Research Fellowship and a grant from the National Institutes of Health (NIH) to W. Earnshaw, and grant GM 29513 from the NIH to D.W. Cleveland, who receives salary support from the Ludwig Institute for Cancer Research.

Submitted: 26 January 2000
Revised: 27 March 2000
Accepted: 30 March 2000

References

Avides, M.C., and D.M. Glover. 1999. Abnormal spindle protein, Asp, and the integrity of mitotic centrosomal microtubule organizing centers. *Science.* 283:1733–1735.

Blangy, A., L. Arnaud, and E.A. Nigg. 1997. Phosphorylation by p34cdc2 protein kinase regulates binding of the kinesin-related motor HsEg5 to the dynactin subunit p150. *J. Biol. Chem.* 272:19418–19424.

Boleti, H., E. Karsenti, and I. Vernos. 1996. Xklp2, a novel *Xenopus* centrosomal kinesin-like protein required for centrosome separation during mitosis. *Cell.* 84:49–59.

Clark, I.B., and D.I. Meyer. 1999. Overexpression of normal and mutant Arp1α (centractin) differentially affects microtubule organization during mitosis and interphase. *J. Cell Sci.* 112:3507–3518.

Compton, D.A., T.J. Yen, and D.W. Cleveland. 1991. Identification of novel centromere/kinetochore-associated proteins using monoclonal antibodies generated against human mitotic chromosome scaffolds. *J. Cell Biol.* 112: 1083–1097.

Compton, D.A., I. Szilak, and D.W. Cleveland. 1992. Primary structure of NuMA, an intranuclear protein that defines a novel pathway for segregation of proteins at mitosis. *J. Cell Biol.* 116:1395–1408.

Dionne, M.A., L. Howard, and D.A. Compton. 1999. NuMA is a component of an insoluble matrix at mitotic spindle poles. *Cell Motil. Cytoskel.* 42:189–203.

Doxsey, S.J., P. Stein, L. Evans, P.D. Calarco, and M. Kirschner. 1994. Pericentrin, a highly conserved centrosome protein involved in microtubule organization. *Cell.* 76:639–650.

Echeverri, C.J., B.M. Paschal, K.T. Vaughan, and R.B. Vallee. 1996. Molecular characterization of the 50-kD subunit of dynactin reveals function for the complex in chromosome alignment and spindle organization during mitosis. *J. Cell Biol.* 132:617–633.

Gaglio, T., A. Saredi, J.B. Bingham, M.J. Hasbani, S.R. Gill, T.A. Schroer, and D.A. Compton. 1996. Opposing motor activities are required for the organization of the mammalian mitotic spindle pole. *J. Cell Biol.* 135:399–414.

Gaglio, T., M.A. Dionne, and D.A. Compton. 1997. Mitotic spindle poles are organized by structural and motor proteins in addition to centrosomes. *J. Cell Biol.* 138:1055–1066.

Gueth-Hallonet, C., J. Wang, J. Harborth, K. Weber, and M. Osborn. 1998. Induction of a regular nuclear lattice by overexpression of NuMA. *Exp. Cell Res.* 243:434–452.

Harborth, J., K. Weber, and M. Osborn. 1995. Epitope mapping and direct visualization of the parallel, in-register arrangement of the double-stranded coiled-coil in the NuMA protein. *EMBO (Eur. Mol. Biol. Organ.) J.* 14: 2447–2460.

Harborth, J., J. Wang, C. Gueth-Hallonet, K. Weber, and M. Osborn. 1999. Self assembly of NuMA: multiarm oligomers as structural units of a nuclear lattice. *EMBO (Eur. Mol. Biol. Organ.) J.* 18:1689–1700.

Hartman, J.J., J. Mahr, K. McNally, K. Okawa, A. Iwamatsu, S. Thomas, S. Cheesman, J. Heuser, R.D. Vale, and F.J. McNally. 1998. Katanin, a microtubule-severing protein, is a novel AAA ATPase that targets to the centrosome using a WD40-containing subunit. *Cell.* 93:277–287.

Heald, R., R. Tournebize, T. Blank, R. Sandaltzopoulos, P. Becker, A. Hyman, and E. Karsenti. 1996. Self-organization of microtubules into bipolar spindles around artificial chromosomes in *Xenopus* egg extracts. *Nature.* 382: 420–425.

Heald, R., R. Tournebize, A. Habermann, E. Karsenti, and A. Hyman. 1997. Spindle assembly in *Xenopus* egg extracts: respective roles of centrosomes and microtubule self-organization. *J. Cell Biol.* 138:615–628.

Holleran, E.A., M.K. Tokito, S. Karki, and E.L. Holzbaur. 1996. Centractin (ARP1) associates with spectrin revealing a potential mechanism to link dynactin to intracellular organelles. *J. Cell Biol.* 135:1815–1829.

Joshi, H.C., M.J. Palacios, L. McNamara, and D.W. Cleveland. 1992. Gamma-tubulin is a centrosomal protein required for cell cycle-dependent microtubule nucleation. *Nature.* 356:80–83.

Kahana, J.A., and D.W. Cleveland. 1999. Beyond nuclear transport. Ran-GTP as a determinant of spindle assembly. *J. Cell Biol.* 146:1205–1210.

Karki, S., and E.L. Holzbaur. 1995. Affinity chromatography demonstrates a direct binding between cytoplasmic dynein and the dynactin complex. *J. Biol. Chem.* 270:28806–28811.

Lydersen, B.K., and D.E. Pettijohn. 1980. Human-specific nuclear protein that associates with the polar region of the mitotic apparatus: distribution in a human/hamster hybrid cell. *Cell.* 22:489–499.

Mattagajasingh, S.N., S.C. Huang, J.S. Hartenstein, M. Snyder, V.T. Marchesi, and E.J. Benz. 1999. A nonerythroid isoform of protein 4.1R interacts with the nuclear mitotic apparatus (NuMA) protein. *J. Cell Biol.* 145:29–43.

McNally, F.J., K. Okawa, A. Iwamatsu, and R.D. Vale. 1996. Katanin, the microtubule-severing ATPase, is concentrated at centrosomes. *J. Cell Sci.* 109: 561–567.

Merdes, A., K. Ramyar, J.D. Vechio, and D.W. Cleveland. 1996. A complex of NuMA and cytoplasmic dynein is essential for mitotic spindle assembly. *Cell.* 87:447–458.

Mitchison, T.J. 1989. Polewards microtubule flux in the mitotic spindle: evidence from photoactivation of fluorescence. *J. Cell Biol.* 109:637–652.

Murray, A.W. 1991. Cell cycle extracts. *In* Methods in Cell Biology, Vol. 36. B.K. Kay and H.B. Peng, editors. Academic Press, San Diego, CA. 581–605.

Quintyne, N.J., S.R. Gill, D.M. Eckley, C.L. Crego, D.A. Compton, and T.A.

Schroer. 1999. Dynactin is required for microtubule anchoring at centrosomes. *J. Cell Biol.* 147:321–334.

Roos, U.P. 1973. Light and electron microscopy of rat kangaroo cells in mitosis. I. Formation and breakdown of the mitotic apparatus. *Chromosoma.* 40:43–82.

Sambrook, J., E.F. Fritsch, and T. Maniatis. 1989. Molecular Cloning. Cold Spring Harbor Laboratory Press, Cold Spring Harbor, NY.

Saredi, A., L. Howard, and D.A. Compton. 1997. Phosphorylation regulates the assembly of NuMA in a mammalian mitotic extract. *J. Cell Sci.* 110:1287–1297.

Sawin, K.E., K. LeGuellec, M. Philippe, and T.J. Mitchison. 1992. Mitotic spindle organization by a plus-end-directed microtubule motor. *Nature.* 359:540–543.

Schafer, D.A., S.R. Gill, J.A. Cooper, J.E. Heuser, and T.A. Schroer. 1994. Ultrastructural analysis of the dynactin complex: An actin-related protein is a component of a filament that resembles F-actin. *J. Cell Biol.* 126:403–412.

Schroer, T.A., and M.P. Sheetz. 1991. Two activators of microtubule-based vesicle transport. *J. Cell Biol.* 115:1309–1318.

Sparks, C.A., E.G. Fey, C.A. Vidair, and S.J. Doxsey. 1995. Phosphorylation of NuMA occurs during nuclear breakdown and not mitotic spindle assembly. *J. Cell Sci.* 108:3389–3396.

Stearns, T., and M. Kirschner. 1994. In vitro reconstitution of centrosome assembly and function: the central role of gamma-tubulin. *Cell.* 76:623–637.

Vaughan, K.T., and R.B. Vallee. 1995. Cytoplasmic dynein binds dynactin through a direct interaction between the intermediate chains and p150 Glued. *J. Cell Biol.* 131:1507–1516.

Waterman-Storer, C.M., S. Karki, and E.L. Holzbaur. 1995. The p150Glued component of the dynactin complex binds to both microtubules and the actin-related protein centractin (Arp-1). *Proc. Natl. Acad. Sci. USA.* 92:1634–1638.

Yang, C.H., E.J. Lambie, and M. Snyder. 1992. NuMA: an unusually long coiled-coil related protein in the mammalian nucleus. *J. Cell Biol.* 116:1303–1317.